INTL JOURNAL OF ELECTRONICS AND TELECOMMUNICATIONS, 2024, VOL. 70, NO. 1, PP. 205-210
Manuscript received October 11, 2023; revised March, 2024. doi: 10.24425/ijet.2024.149532

Method of assessing the information reliability of in 5G wireless transmission systems

Vladyslav Vasylenko, Serhii Zaitsev, Yuliia Tkach, Oleksandr Korchenko, Ruslana Ziubina, Olga Veselska

***Abstract*—The article proposes a method of assessing information transmission reliability by using the output normalized logarithmic ratio of the likelihood function (LRLF) of the decoder. Based on the evaluation, the method allows adapting system parameters with turbo codes (TC) or LDPC code. This method can be used in combination with other methods of parametric and structural adaptation using turbo codes or LDPC codes.**

***Keywords*—logarithmic ratio of the likelihood function; turbo codes; LDPC-codes**

I. Introduction

THE development and use of mobile networks of the fifth generation 5G [1,2] (5G/IMT-2020 standard) gave a rapid impetus to the further development of various fields.
It is the increase in data transmission speed and the increase in network capacity that open up new prospects for their use in industry and the corporate segment.

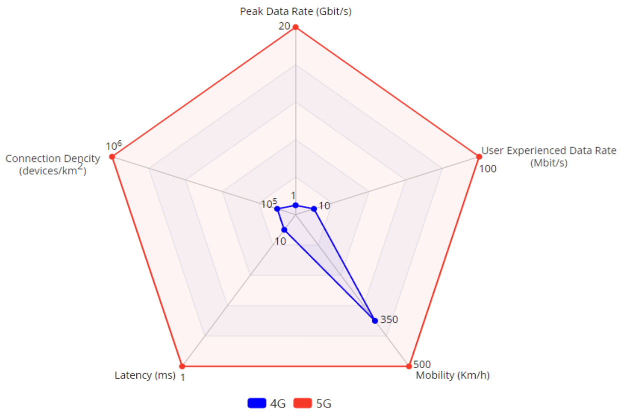

Fig. 1. Comparative characteristics of 5G and 4G system

From fig. 1 we can see that 5G has significant advantages over 4G, namely:

- a 10-fold increase in the average user data transfer speed;
- increase in user mobility by 42%;
- a 20-fold increase in peak data transfer speed;
- reduction of signal delays by 10 times;
- increasing the density (number) of devices by 10 times per square kilometer.

Let's consider in more detail how the fifth generation 5G mobile networks impact the development of various fields and technologies.

5G and the Internet of Things (IoT)

The development of mobile networks of the fifth generation 5G has become an important factor in the development of IoT. A significant increase in the number of devices in applications with IoT technology requires extensive opportunities for fast data transmission, low signal delay, security and reliability in data transmission. Most of these criteria are solved by 5G [4].

Also, an important aspect for the use of 5G in IoT is the technology of dividing the radio network into separate "layers", which allows you to divide different types of devices into segments that do not intersect with each other and thus provide them with distributed access. This is important when implementing "Smart Home", "Smart City" or when used in industrial IoT

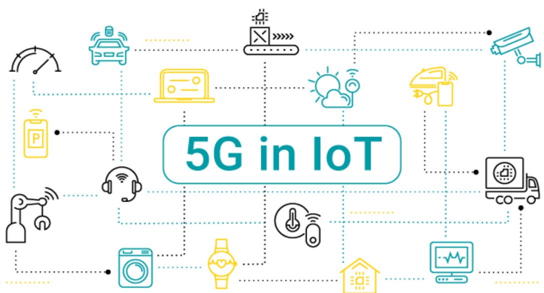

Fig. 2. Use of 5G in IoT

The development of IoT, in turn, gives a powerful impetus to the rapid implementation of Industry 4.0 [5], as well as digital doubles [6, 7]. In fig. 3 shows an example of a digital double.

First Author is with the Institute of Telecommunications and Global Information Space of the National Academy of Sciences of Ukraine, Kyiv, Ukraine, (e-mail: vladvasilenko9@gmail.com).
Second Author is with the University of Technology, Kielce, Poland, (e-mail: szaitsev@tu.kielce.pl).
Third Authors is with Chernihiv Polytechnic National University, Chernihiv, Ukraine, (e-mail: tkachym79@gmail.com).
Forth Author is with Department of Information Technology Security of National Aviation University, Kyiv, Ukraine, (e-mail: agkorchenko@gmail.com).
Fifth and Sixth Authors are with Department of Computer Science and Automatics of the University of Bielsko-Biala, Bielsko-Biala, Poland, (e-mail: rziubina@ath.bielsko.pl, oveselska@ath.bielsko.pl).

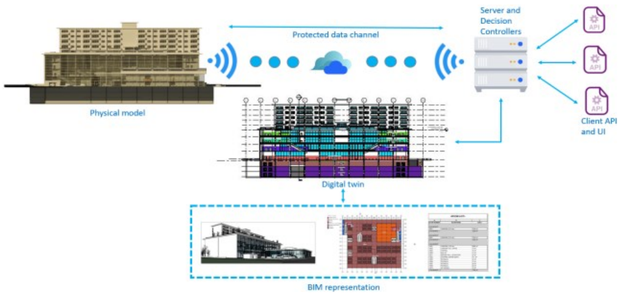

Fig. 3. General diagram of a digital double of a building using IoT

Important components of this digital double scheme are means of measuring various characteristics (for example, temperature, etc.), as well as means of processing and transmitting data and means of making decisions based on the received information. But one of the main tasks when using IoT is to assess and ensure the credibility and reliability of data transmission.

Information transmission reliability can be ensured by the use of turbo codes [8] and LDPC codes [9, 10], which are adopted by the standards of 5G mobile networks.

II. Analysis of Research and Publications

The method of data decoding and channel estimation is proposed in work [11]. The proposed scheme is based on the parallel concatenation of two systematic recursive convolutional codes with puncturing. The disadvantages of this method are the presence of redundant symbols, and this method is inferior to traditional schemes in the area of minimum error.

In work [12], a method for estimating LRLF is proposed. The disadvantage of this method is that it is effective only for high-performance systems with low latency, using neural networks.

An iterative receiver for a channel with phase-coherent fading is presented in work [13]. The receiver evaluates the channel and decodes the LDPC code using a product-of-sum algorithm. The disadvantage of this method is the high calculation complexity of the iterative evaluation of the channel.

III. Formulating the Goals of the Article

The purpose of the article is to develop a method for assessing information transmission reliability by using the output normalized logarithmic ratio of the likelihood function (LRLF) of the decoder. Based on the evaluation, the method allows adapting system parameters with TC or LDPC code.

IV. Presentation of the Main Material

Let's consider how the LRLF is calculated at the output of the TC decoder. LRLF $L(x)$ about the transmitted bit x looks like[14, 15]:

$$L(x) = L_c(x) + L_a(x) + L_e(x), \qquad (1)$$

where $L_c(x)$ - channel information, $L_a(x)$ and $L_e(x)$ respectively, a priori and a posteriori LRLF about the transmitted bit. If $L(x) \geq 0$, then a decision is made that a bit with a value of 1 was transmitted, otherwise 0.

The structural diagram of the modified turbo code iterative decoder with the block of the module for calculating the normalized number of changes in the sign of posterior-prior LRLF F* is shown in Fig. 4, where I is an interleaver, D is a deinterleaver, $F^{d,j}$ – displacement modulesign changes $L_a(x)$ / $L_e(x)$ for iteration j of decoder d, F^{Σ} – a module for calculating the sum of the number of changesign $L_a(x)$ / $L_e(x)$ for all iterations and decoders,F*– a module for calculating the normalized number of changes in the sign of a posteriori-apriori LRLF.

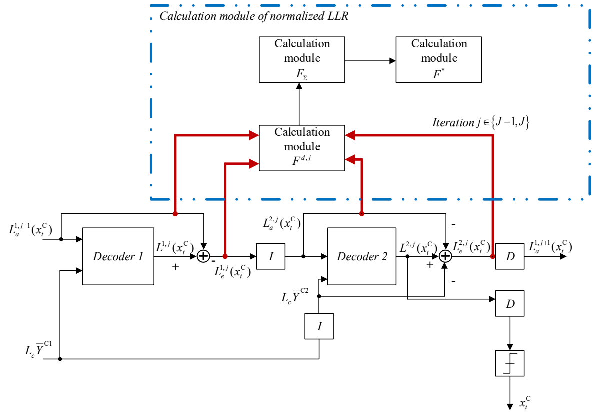

Fig. 4. Structural diagram of the modified TC iterative decoder

In fig. 5 presents the structural one scheme module for calculating the normalized number of changes in the sign of posterior-prior LRLF F*.

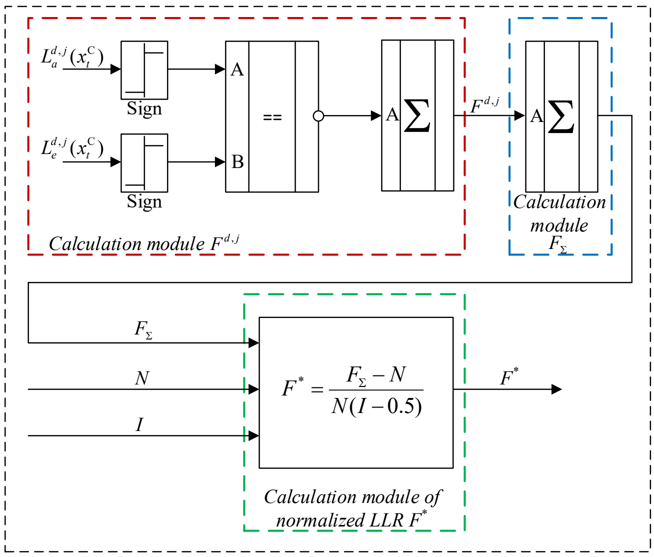

Fig. 5. Structural diagram module for calculating the normalized number of changes in the sign of posterior-prior LRLF F*

At the input of the calculation module $F^{d,j}$ a priori and a posteriori LRLF are received $L_a^{d,j}(x_t^C)$ and $L_e^{d,j}(x_t^C)$, then their signs are compared and if they are not equal, then the values $F^{d,j}$ increases by 1:

$$F^{d,j} = F^{d,j} + 1, \quad \text{if } \operatorname{sign}\left(L_a^{d,j}(x_t^{C})\right) \neq \operatorname{sign}\left(L_e^{d,j}(x_t^{C})\right), \quad t \in \overline{1,N}, \qquad (2)$$

where N is the number of bits in the block.

The more often the sign changes $L_a^{d,j}(x_t^{C}) / L_e^{d,j}(x_t^{C})$, the more often this leads to a deterioration in the reliability of data transmission.

In fig. 6 shows an example of changing the sign of posterior-prior LRLFs depending on the values of the signal-to-noise ratio (SNR). The simulation was carried out for N = 1000 bits, the decoding algorithm was LOG-MAP, the interleaver was pseudo-random, and the number of iterations was I = 8.

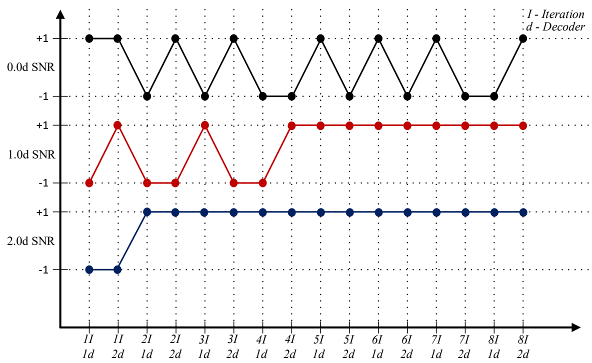

Fig. 6. An example of changing the sign of posterior-prior LRLFs depending on the values of the signal/noise ratio

As we can see, the larger the LVDS, the fewer sign changes occur and the fewer errors during data transmission.

Total number of sign changes $L_a^{d,j}(x_t^{C}) / L_e^{d,j}(x_t^{C})$ for all decoding iterations F_Σ is calculated by the formula:

$$F_\Sigma = \sum_{j=1}^{I} \sum_{d=1}^{2} F^{d,j}. \qquad (3)$$

The normalized value of the number of changes in the sign of posterior-prior LRLF is calculated according to the formula:

$$F^* = \frac{F_\Sigma - N}{N(I - 0.5)} \qquad (4)$$

The value is within the range $F^* \in [0,1]$. If F* =1, then the transmission channel affects the transmitted information and correct decoding is not possible, if F* = 0, then the transmission channel does not affect the non-transmitted information. In fig. 7 presents a graph of the dependence of the efficiency of the data transmission system on the normalized valuethe number of changes in the sign of posterior-prior LRLFs.

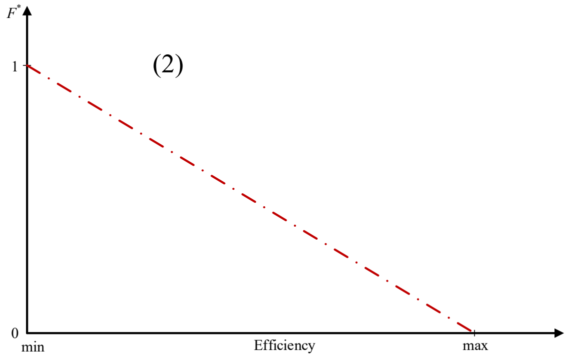

Fig. 7. Ggraph of the dependence of the efficiency of the data transmission system on the normalized value the number of changes in the sign of posterior-prior LRLFs

V. Analysis of the Results

Simulation modeling has been conducted to analyze the results. The simulation was carried out in the Visual Studio 2022 environment. A data transmission system with turbo codes, a channel with additive white Gaussian noise, a module for calculating the probability of a decoding error and a module for calculating the normalized LRLF has been implemented.

A turbo code with a polynomial (1, 7/5), decoding algorithms LOG-MAP, MAX-LOG-MAP, MAP, coding rate R = 1/3, pseudorandom and regular interleavers (deinterleavers), number of bits in the block N = 100 400, 1000 was used. The signal-to-noise ratio varied from 0 to 1.6 dB.

We will also calculate the ratio of the values of the normalized LRLF to the probability of a bit error in order to estimate the number of errors as a result of using this method:

$$\Delta = \frac{F^*}{P_B} \qquad (5)$$

Value Δ = 1 means that the assessment of information reliability according to the proposed method coincides with the assessment of the reliability of the ideal assessment, if Δ > 1, then this means that the number of errors is greater in Δ times with the proposed evaluation method. If Δ < 1, then in this case the number of detected errors is less than the ideal estimate.

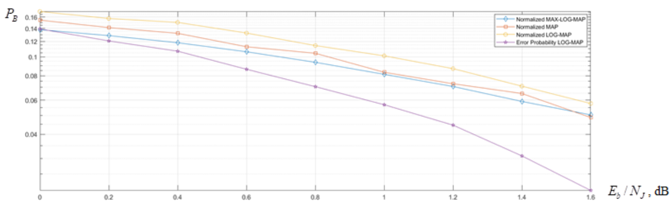

Fig. 8. Graph of the probability of error and the normalized logarithmic ratio of the likelihood function (LRLF) depending on the SNR (signal to noise ratio) (N = 100 bits in the block, the interleaver is regular, I = 4)

Value Δ for N = 100 bits in a block, the interleaver is regular, I = 4 (according to the data in Fig. 8) vary from 0.9913 to 2.443.

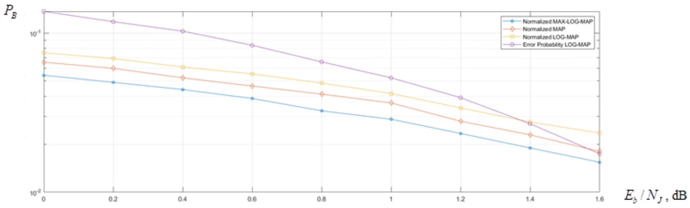

Fig. 9. Graph of the probability of error and the normalized logarithmic ratio of the likelihood function (LRLF) depending on the SNR (N = 100 bits in the block, interleaver – regular, I = 8)

Value Δ for N = 100 bits in a block, the interleaver is regular, I = 8 (according to the data in Fig. 9) vary from 0.5496 to 1.3506.

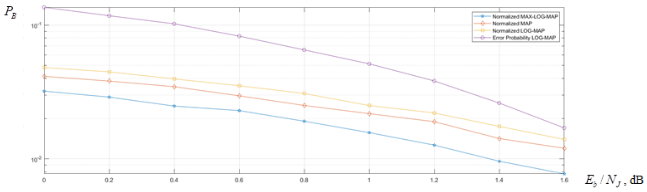

Fig. 10. Graph of the probability of error and the normalized logarithmic ratio of the likelihood function (LRLF) depending on the SNR (N = 100 bits in the block, interleaver – regular, I = 12)

Value Δ for N = 100 bits in a block, the interleaver is regular, I = 12 (according to the data in Fig. 10) vary from 0.3547 to 0.8204.

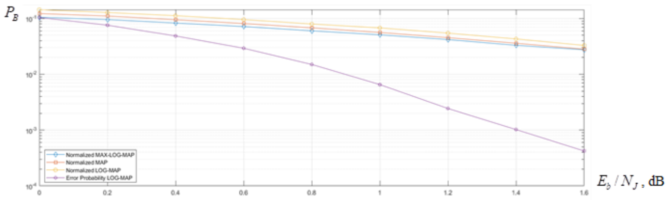

Fig. 11. Graph of the probability of error and the normalized logarithmic ratio of the likelihood function (LRLF) depending on the SNR (N = 400 bits in a block, interleaver – regular, I = 4)

Value Δ for N = 400 bits in a block, the interleaver is regular, I = 4 (according to the data in Fig. 11) vary from 1.3784 to 77.7971.

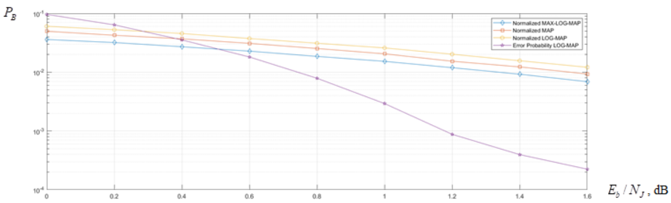

Fig. 12. Graph of the probability of error and the normalized logarithmic ratio of the likelihood function (LRLF) depending on the SNR (N = 400 bits in a block, interleaver – regular, I = 8)

Value Δ for N = 400 bits in a block, the interleaver is regular, I = 8 (according to the data in Fig. 12) vary from 0.6271 to 54.2853.

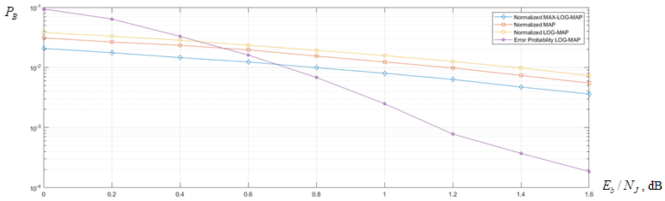

Fig. 13. Graph of the probability of error and the normalized logarithmic ratio of the likelihood function (LRLF) depending on the SNR (N = 400 bits in a block, interleaver – regular, I = 12)

Value Δ for N = 400 bits in a block, the interleaver is regular, I = 12 (according to the data in Fig. 13) vary from 0.4047 to 39.4771.

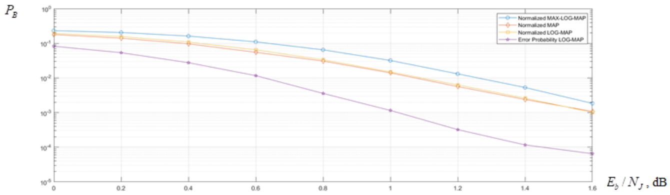

Fig. 14. Graph of the probability of error and the normalized logarithmic ratio of the likelihood function (LRLF) depending on the SNR (N = 1000 bits in a block, interleaver – pseudorandom, I = 4)

Value Δ for N = 1000 bits in a block, the interleaver is pseudorandom, I = 4 (according to the data in Fig. 14) vary from 2.3376 to 15.6374.

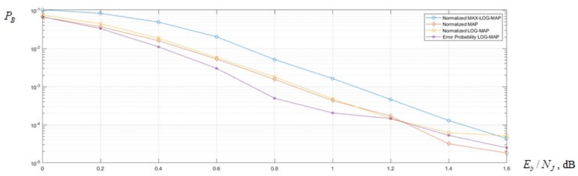

Fig. 15. Graph of the probability of error and the normalized logarithmic ratio of the likelihood function (LRLF) depending on the SNR (N = 1000 bits in the block, the interleaver is pseudo-random, I = 8)

Value Δ for N = 1000 bits in a block, the interleaver is pseudo-random, I = 8 (according to the data in Fig. 15) vary from 1.1134 to 2.064.

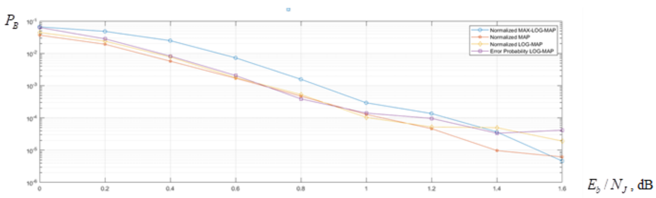

Fig. 16. Graph of the probability of error and the normalized logarithmic ratio of the likelihood function (LRLF) depending on the SNR (N = 1000 bits in a block, interleaver – pseudorandom, I = 12)

Value Δ for N = 1000 bits in a block, the interleaver is pseudo-random, I = 12 (according to the data in Fig. 16) vary from 0.462 to 1.367.

pAnalysis of simulation results shows that the proposed estimation method reliability of information is more effective when using a pseudo-random interleaver and blocks of long length in the turbo code structure ($\Delta \rightarrow 1$), when using a regular interleaver and blocks of small length, the efficiency of the method is much reduced.

Figures 8-16 show the dependence of the probability of a bit error and the normalized value of LRLF on the signal-to-noise ratio. Analysis of the simulation results shown in fig. 8-6 suggests that as the size of the data block increases from N = 100 to 1000 bits and the number of decoding iterations increases, the curve of the normalized value of LRLF approaches the curve of the decoding error probability. By values Δ we can see that using the normalized value of LRLF to estimate the probability, more errors are detected. But using this evaluation method, we do not need to use an additional channel, which gives a gain in bandwidth. Based on the simulation results, tables with bit error probabilities (tables I, II) and normalized values of LRLF (tables III, IV) have been obtained. These table values can be used to evaluate the quality of the channel.

TABLE I
PROBABILITY OF BIT ERROR DURING TURBO CODING WITH REGULAR INTERLEAVING ALGORITHM, MAX-LOG-MAP DECODING ALGORITHM, WITHOUT PERFORATION AT 1, 2, 4, 8TH ITERATIONS, THE NUMBER OF BITS IN THE BLOCK IS 100 BITS.

VSSH/Iteration	1	2	4	8
0	0.19208	0.20048	0.19173	0.18498
0.2	0.1797	0.185053	0.17527	0.16695
0.4	0.16588	0.173771	0.16652	0.15359
0.6	0.15735	0.158248	0.14514	0.14696
0.8	0.14488	0.143338	0.13742	0.12906
1.0	0.12945	0.127717	0.11543	0.11345
1.2	0.11449	0.114083	0.10316	0.09547
1.4	0.10349	0.100446	0.09167	0.08751
1.6	0.09516	0.086012	0.07454	0.0733
1.8	0.0837	0.073047	0.06557	0.06016
2.0	0.07264	0.061378	0.0524	0.04882
2.2	0.05957	0.050349	0.04099	0.04073
2.4	0.05099	0.041354	0.03436	0.02971

TABLE II
THE PROBABILITY OF A BIT ERROR DURING TURBO CODING WITH A PSEUDO-RANDOM INTERLEAVING ALGORITHM, THE MAX-LOG-MAP DECODING ALGORITHM, WITHOUT PERFORATION AT 1, 2, 4, 8 ITERATIONS, THE NUMBER OF BITS IN THE BLOCK IS 1000 BITS

VSSH/Iteration	1	2	4	8
0	0.16059	0.148932	0.141715	0.14901
0.2	0.14033	0.124743	0.105955	0.10578
0.4	0.12576	0.094734	0.066927	0.04612
0.6	0.11006	0.069667	0.03502	0.00305
0.8	0.09443	0.047556	0.01382	0.002983
1.0	0.07558	0.029731	0.00607	0.000493
1.2	0.06486	0.015605	0.001136	0.0001358
1.4	0.05013	0.008243	0.000353	0.0000872
1.6	0.03741	0.003851	0.000097	0.0000324
1.8	0.02712	0.001494	0.000033	0.000015
2.0	0.0183	0.000721	0.000024	0.0000096
2.2	0.01396	0.0002	0.000011	0.000004
2.4	0.00864	0.00013	0.000004	0.0000017

TABLE III
NORMALIZED VALUES OF LRLF DURING TURBO CODING WITH REGULAR INTERLEAVING ALGORITHM, MAX-LOG-MAP DECODING ALGORITHM, WITHOUT PERFORATION AT 1, 2, 4, 8TH ITERATIONS, THE NUMBER OF BITS IN THE BLOCK IS 100 BITS

VSSH/Iteration	1	2	4	8
0	77.055	39,833	13.957	5.421
0.2	75.115	37.435	12.693	4.869
0.4	72,899	35,795	11.551	4.387
0.6	68,789	32.861	10.644	3.907
0.8	65.224	30.402	9.340	3.418
1.0	61.513	27.722	8.232	2.807
1.2	57.511	24,928	6.873	2.373
1.4	53.407	21.915	5.813	1.888
1.6	49.420	19.394	4.826	1.534
1.8	45.169	16.687	3,800	1.134
2.0	40.738	14.079	2.990	0.843
2.2	37.090	11.551	2.354	0.630
2.4	33.434	9.646	1.661	0.427

TABLE IV
NORMALIZED VALUES OF LRLF DURING TURBO CODING WITH PSEUDO-RANDOM INTERLEAVING ALGORITHM, MAX-LOG-MAP DECODING ALGORITHM, WITHOUT PERFORATION AT 1, 2, 4, 8 ITERATIONS, THE NUMBER OF BITS IN THE BLOCK IS 1000 BITS

SNR/Iteration	1	2	4	8
0	87.954	56.460	23.339	10.410
0.2	84,995	53.260	20.503	8.260
0.4	82.179	48,855	16.496	5.136
0.6	78.096	43.724	11.397	2.107
0.8	74.258	37,545	6.624	0.591
1.0	69.094	31.349	3.170	0.192
1.2	64.532	25.018	1.346	0.036
1.4	58.835	19.010	0.516	0.014
1.6	53.010	14.084	0.190	0.003
1.8	47.408	10.081	0.076	0.001
2.0	41.624	7.216	0.025	5.41e-04
2.2	36.308	4.885	0.013	1.27e-04
2.4	31.592	3.355	0.004	6.12e-05

The degree of similarity between the normalized value of LRLF and the probability of a bit error will be estimated using the correlation function. Fig. 17 shows the dependence of the correlation coefficient on the signal/noise ratio in the channel for N = 1000 and I = 2, 4, 8, 12.

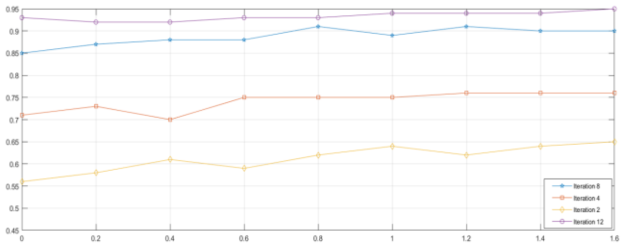

Fig. 17. Graph of the dependence of the correlation coefficient on the signal-to-noise ratio in the channel for N = 1000 and different decoding iterations

The analysis shows that with an increase in the number of decoding iterations, the accuracy of the assessment of the reliability of information increases, so for 12 iterations the values of the correlation coefficient change from 92 to 95%, for 8 iterations - from 85 to 90%, for 4 iterations - from 71 to 76%, for 2 iterations of decoding - from 56 to 65%.

VI. Conclusions

1. The article proposes a method of assessing information transmission reliability by using the output normalized LRLF decoder. Based on the value of the output normalized LRLF of the decoder, it is possible to decide on the adaptation of systems with a turbo code or an LDPC code.

2. Analysis of the simulation results shows that with an increase in the size of the data block from N = 100 to 1000 bits and an increase in the number of decoding iterations, the curve of the normalized value of LRLF approaches the ideal curve of the decoding error probability. This allows assessing the quality of the channel in real time and make a decision to change certain parameters of the system, depending on the value of the normalized LRLF.

3. This method can be used in combination with other methods of parametric and structural adaptation using turbo codes or LDPC codes.

References

[1] Adebusola JA, Ariyo AA, Elisha OA, Olubunmi AM, Julius OO, "An Overview of 5G Technology," 2020 International Conference in Mathematics, *Computer Engineering and Computer Science* (ICMCECS). - 2020. - P. 1-4. doi:10.1109/ICMCECS47690.2020.240853

[2] Mansoor Shafi, Andreas F. Molisch, Peter J Smith, Thomas Haustein, Peiying Zhu, Prasan De Silva, Fredrik Tufvesson, Anass Benjebbour, Gerhard Wunder "5G: A Tutorial Overview of Standards, Trials, Challenges, Deployment and Practice,", *IEEE Journal on Selected Areas in Communications*. - 2017. - Vol. 35, no. 6. – P. 1201-1221. doi:10.1109/JSAC.2017.2692307

[3] Hazarika, A.; Rahmati, M., "Towards an Evolved Immersive Experience: Exploring 5G- and Beyond-Enabled Ultra-Low-Latency Communications for Augmented and Virtual Reality," *Sensors* 2023, 23, 3682. doi:10.3390/s23073682

[4] Li, S., Xu, LD, & Zhao, S. (2018). "5G Internet of Things: A survey," *Journal of Industrial Information Integration*, 10, 1-9. doi:10.1016/j.jii.2018.01.005

[5] Alhayani, B., Kwekha-Rashid, AS, Mahajan, HB et al. "5G standards for the Industry 4.0 enabled communication systems using artificial intelligence: perspective of smart healthcare system," Appl Nanosci 13, 1807–1817 (2023). doi:10.1007/s13204-021-02152-4

[6] M. Sanz Rodrigo, D. Rivera, JI Moreno, M. Álvarez-Campana and DR López, "Digital Twins for 5G Networks: A Modeling and Deployment Methodology," in *IEEE Access*, vol. 11, pp. 38112-38126, 2023, doi:10.1109/ACCESS.2023.3267548

[7] HX Nguyen, R. Trestian, D. To and M. Tatipamula, "Digital Twin for 5G and Beyond," in *IEEE Communications Magazine*, vol. 59, no. 2, pp. 10-15, February 2021, doi:10.1109/MCOM.001.2000343

[8] Arora K., Singh J., Randhawa YS, "A survey on channel coding techniques for 5G wireless networks", *Telecommun. Syst*. - 2020. - Vol. 73 – P. 637–663.

[9] J. Bae & A. Abotabl, HP Lin, KB Song, J. Lee, "An overview of channel coding for 5G NR cellular communications," *APSIPA Transactions on Signal and Information Processing*, 2019, p. 1-14. doi:10.1017/ATSIP.2019.10

[10] MacKay DJC, Near RM, "Shannon limit performance of low density parity check codes," *Electron. Lett*., 1996, Vol. 32, no. 18, p. 457–458.

[11] Takeuchi K. A, Muller RR, Vehkapera M., "Construction of Turbo-Like Codes for Iterative Channel Estimation Based on Probabilistic Bias," 2011 *IEEE Global Telecommunications* Conference - GLOBECOM 2011, 2011, p. 1-5. doi:10.1109/GLOCOM.2011.6133738

[12] Arvinte M., Tewfik AH, Vishwanath S., "EQ-Net: Joint Deep Learning-Based Log-Likelihood Ratio Estimation and Quantization," ArXiv,abs/2012.12843v2.

[13] Jin X., Eckford AW, Fuja TE, "Analysis of Joint Channel Estimation and LDPC Decoding on Block Fading Channels," International Symposium on Information Theory and its Applications, ISITA2004 Parma, Italy, October 10–13. – 2004. P. 679 – 684.

[14] 14. Berrou C., "Codes and Turbo Codes", *Springer*, 2010. - 415 p.

[15] Vucetic B., Yuan J., "Turbo Codes," Principles and Applications, *Springer Science*, 2000. - 307 p.